Supplementary Information

Metal-Organic Framework-Derived Hierarchical Ultrathin CoP nanosheets for Overall Water Splitting

*Jianglin Liu [a], Yan Gao [a], Xinxin Tang [a], Ke Zhan [a], Bin Zhao [a], Bao Yu Xia [b], Ya Yan [a,] **

[a] School of Materials Science & Engineering, University of Shanghai for Science and Technology, 516 Jungong Road, Shanghai 200093, PR China

[b] Key laboratory of Material Chemistry for Energy Conversion and Storage (Ministry of Education), Hubei Key Laboratory of Material Chemistry and Service Failure, School of Chemistry and Chemical Engineering, Wuhan National Laboratory for Optoelectronics, Huazhong University of Science and Technology (HUST), 1037 Luoyu Road, Wuhan 430074, PR China

Corresponding author. E-mail: yanya@usst.edu.cn (Y. Yan)

Experimental details

Materials and Chemicals: Nickel(II) nitrate hexahydrate ($Ni(NO_3)_2 \cdot 6H_2O$), cobalt(II) nitrate hexahydrate($Co(NO_3)_2 \cdot 6H_2O$), sodium hypophosphite monohydrate ($NaH_2PO_2 \cdot H_2O$), 2-methylimidazole (2-MeIm) and potassium hydroxide were purchased from Adamas Reagent Co., Ltd. Nickel foam (thickness: 1.6 mm) was obtained from CeTech Co., Ltd. Commercial Pt/C catalyst (20 wt%) were bought from Johnson Matthey Company (Shanghai, China). IrO_2 and nafion (5 % wt.) were obtained from Afar Aesar. All chemicals were used without further purification.

Synthesis of Co-MOF/NF: In a typical fabrication procedure, 2 mmol $Co(NO_3)_2 \cdot 6H_2O$ and 16 mmol 2-MeIm were dissolved in 40 mL deionized water to form two clear solution, respectively. Then, the solution of 2-MeIm was subsequently poured into the solution of $Co(NO_3)_2 \cdot 6H_2O$ with a piece of clean Ni foam, which was kept at room temperature for 3 h. The reacted sample with blue color was taken out and washed with

methanol several times, and dried at 60 °C to obtain Co-MOF precursor. To perform the the concentration-dependent experiments, the molar ratio of $Co(NO_3)_2 \cdot 6H_2O$ and 2-MeIm was tuned at 1:4 and 1:16 to instead the original one (1:8) , respectively (Figure S2).

Synthesis of hierarchical $Co(OH)_2$/NF: A piece of Co-MOF/NF was immersed into an ethanol solution (100 mL) containing $Co(NO_3)_2 \cdot 6H_2O$ (3 mmol) with stirring for 30 min. The obtained $Co(OH)_2$ sample was then taken out, washed with ethanol, and dried in 60 °C. To perform the etching time-dependent experiments, a series of etching time including 0, 10, and 60 min were employed.

Synthesis of hierarchical CoP/NF: In the typical synthesis procedure, a piece of $Co(OH)_2$/NF intermediate and $NaH_2PO_2 \cdot H_2O$ (0.1 g) were placed at the downstream and upstream sides of the tube furnace, respectively. Then the samples were heated at 300 °C for 60 min with a heating speed of 2 °C/min under Ar atmosphere. Noted that the mass loading of active material of pure CoP on NF is about 2.1 mg cm^{-2}. To perform the temperatures-dependent experiments, the different annealing temperatures including 250 and 350 °C were employed. For comparison, all intermediates with different etching time were thermal-annealed under the same conditions.

Synthesis of L-CoP/NF: The large-size cobalt hydroxide precursors (L-$Co(OH)_2$) were grown by electrodeposition in $Co(NO_3)_2$ aqueous solution(2 mmol 100 mL) with a three-electrode system. a piece of nickle foam (1*2 cm), a platinum plate and a Ag/AgCl were used as working electrode, counter electrode and reference electrode, respectively. The electrodeposition of cobalt hydroxide was performed at room temperature applying a constant potential of -1.0 V (vs. Ag/AgCl). After deposition for 5 min, the resulting green sample was carefully rinsed several times with deionized water, and finally dried at 60 °C. The L-CoP/NF sample was prepared by the same phosphidation method as described above, except that the precursor was L-$Co(OH)_2$/NF.

Materials characterization: The morphologies were characterized with field-emission scanning electron

microscopy (FE-SEM, Quanta FEG450) and transmission electron microscopy (TEM, FEI, TECNAI F30). The elemental composition and distribution was investigated with Energy dispersive X-ray spectroscopy (EDX, JEOL-2010) attached to the FE-SEM. The surface structure of the composites was characterized by An Autosorb IQ Gas Sorption System at 77 K. X-ray diffraction (XRD) spectrum was measured by Bruker D8-Advance X-ray diffractometer with Cu Ka radiation to analyze crystal structure of the samples. The Raman spectrum of as-prepared samples was conducted with a LabRAM HR 800 system at 532 nm laser. FT-IR spectra were recorded in the range of 4000–450 cm^{-1} with a 92 JASCO FT/IR-460 spectrophotometer. X-ray photoelectron spectroscopy (XPS, ESCALAB250Xi, Thermo) was carried out to analyze chemical composition and valence states of the constituent elements in the samples.

Electrochemical measurement: All electrochemical measurement was performed in a standard three-electrode system on CHI760E electrochemical workstation (Chenhua, shanghai), while using the as-obtained catalysts on NF as the working electrode, a carbon rod as the counter electrode, and an Ag/AgCl as the reference electrode. 1 M KOH, 1 M PBS and 0.5 M H_2SO_4 were employed as the electrolyte solution. For HER, the linear sweep voltammograms (LSVs) were measured in a potential range of 0 to -0.5 V vs RHE at a scan rate of 5 mV s^{-1}, while for OER, the LSVs were obtained from 1.0 to 1.8 V vs RHE at a scan rate of 2 mV s^{-1}. Electrochemical impedance spectroscopy (EIS) was measured in the frequency range of 0.01 Hz to 100 kHz with a 5 mV AC dither for HER and OER, respectively. Cyclic voltammograms (CVs) were tested at different scan rates, which are employed to estimate the double-layer capacitances (C_{dl}) of the catalysts. Chronopotentiometry curves were obtained with a constant current density at 10 mA cm^{-2}. Overall water splitting performance was evaluated in a two-electrode system by using CoP/NF as the catalysts for HER and OER in 1 M KOH. And the polarization curves were recorded at a scan rate of 2 mV s^{-1}. All potentials reported in this paper were converted from vs. Ag/AgCl to vs. RHE by adding a value of 0.197 + 0.059*pH, and were corrected for ohmic losses.

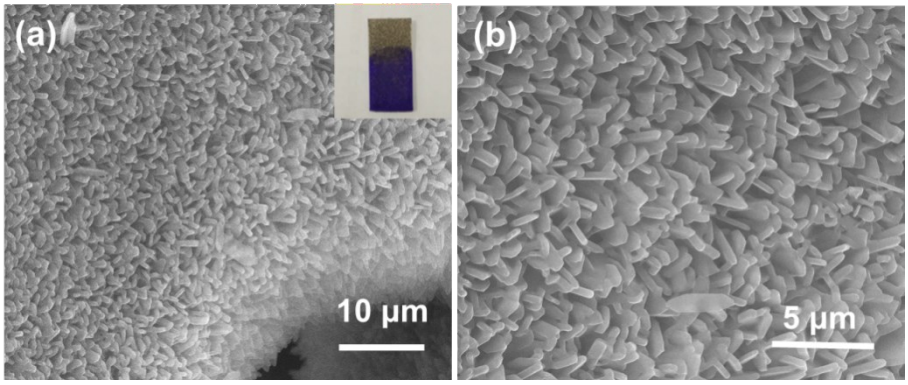

Figure S1. SEM images of Co-MOF (Co^{2+}/2-MeIm : 1/8).

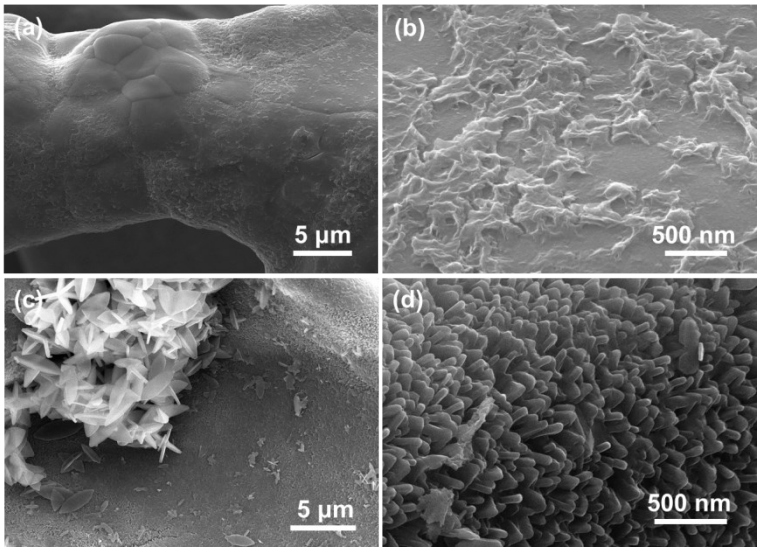

Figure S2. SEM images of Co-MOF with the different Co^{2+}/2-MeIm molar ratio: (a,b) 1:4; (c,d) 1:16.

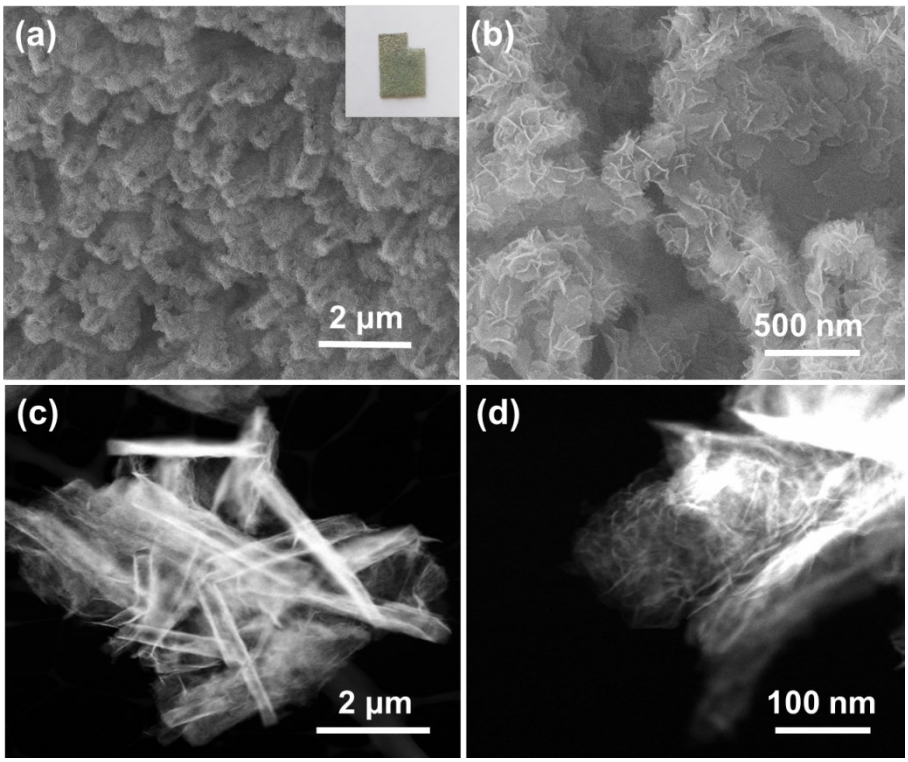

Figure S3. (a, b) SEM images and (c, d) TEM images of $Co(OH)_2$.

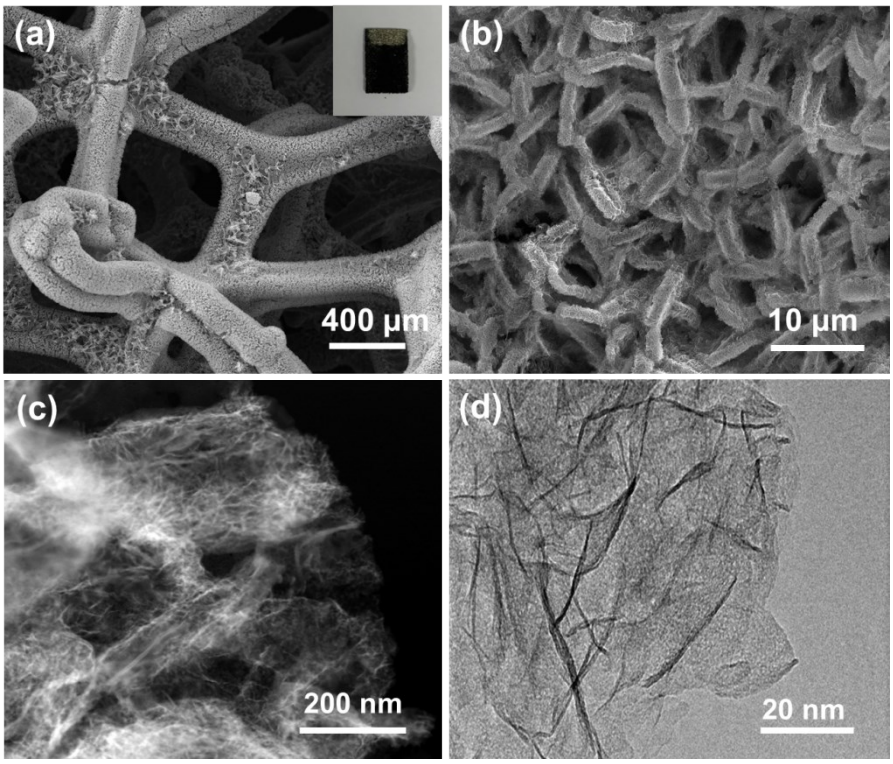

Figure S4. (a, b) SEM images and (c, d) TEM images of CoP.

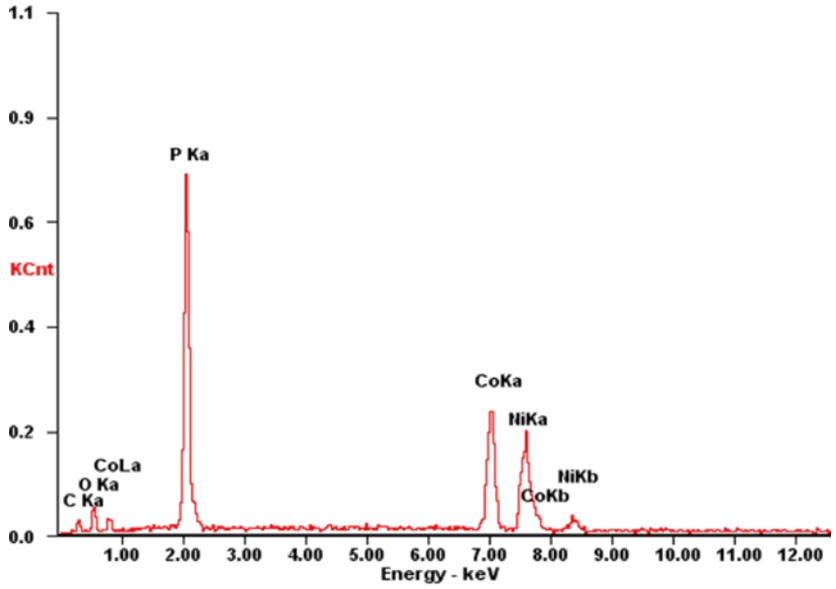

Figure S5. EDX spectra of pure CoP.

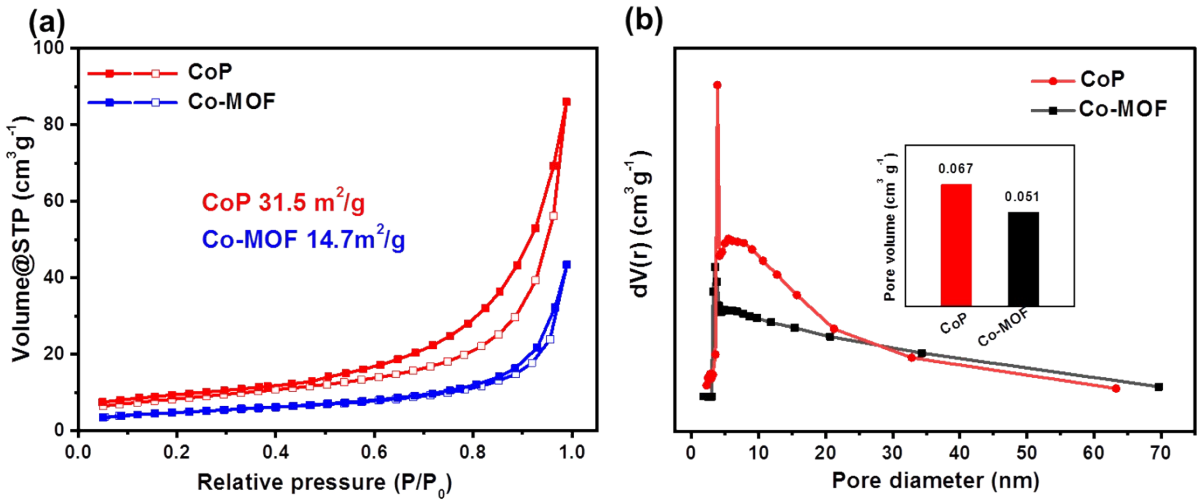

Figure S6. (a) N_2 adsorption−desorption isotherms and (b) the pore size distribution curves of CoP and Co-MOF. Inset in Figure S4b: pore volumes of CoP and Co-MOF sample.

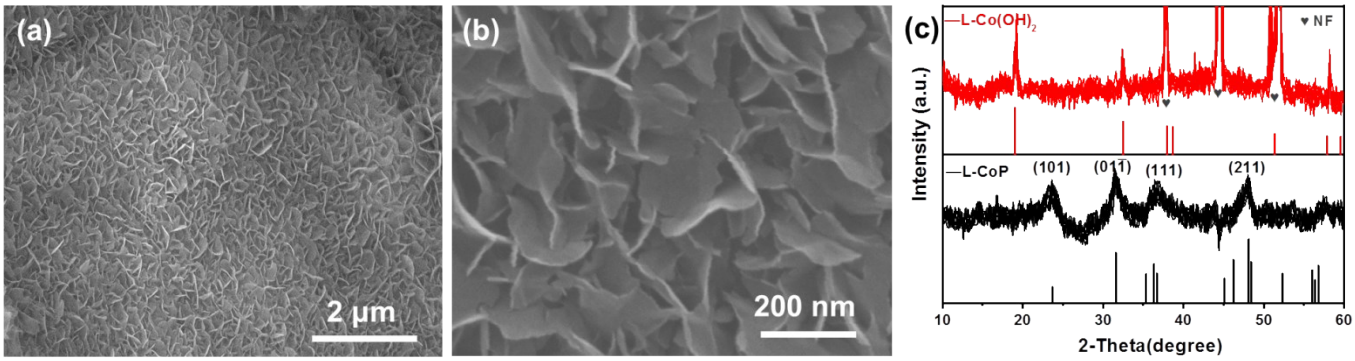

Figure S7. (a, b) SEM images of L-CoP/NF, and (c) XRD pattern of L-Co(OH)$_2$ and L-CoP.

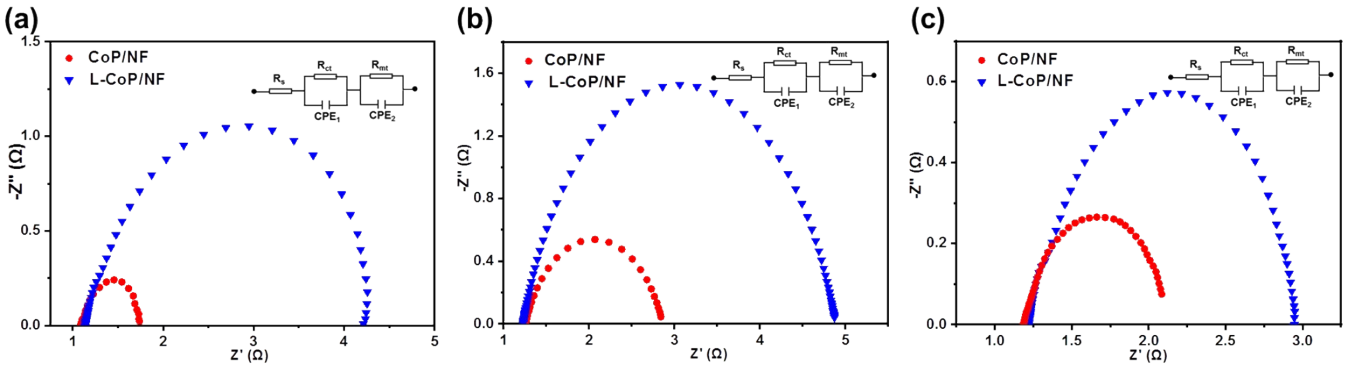

Figure S8. Nyquist plots of the as-synthesized CoP/NF and L-CoP/NF catalysts in (a) 1M KOH, (b) 1 M PBS and (c) 0.5 M H_2SO_4 for HER.

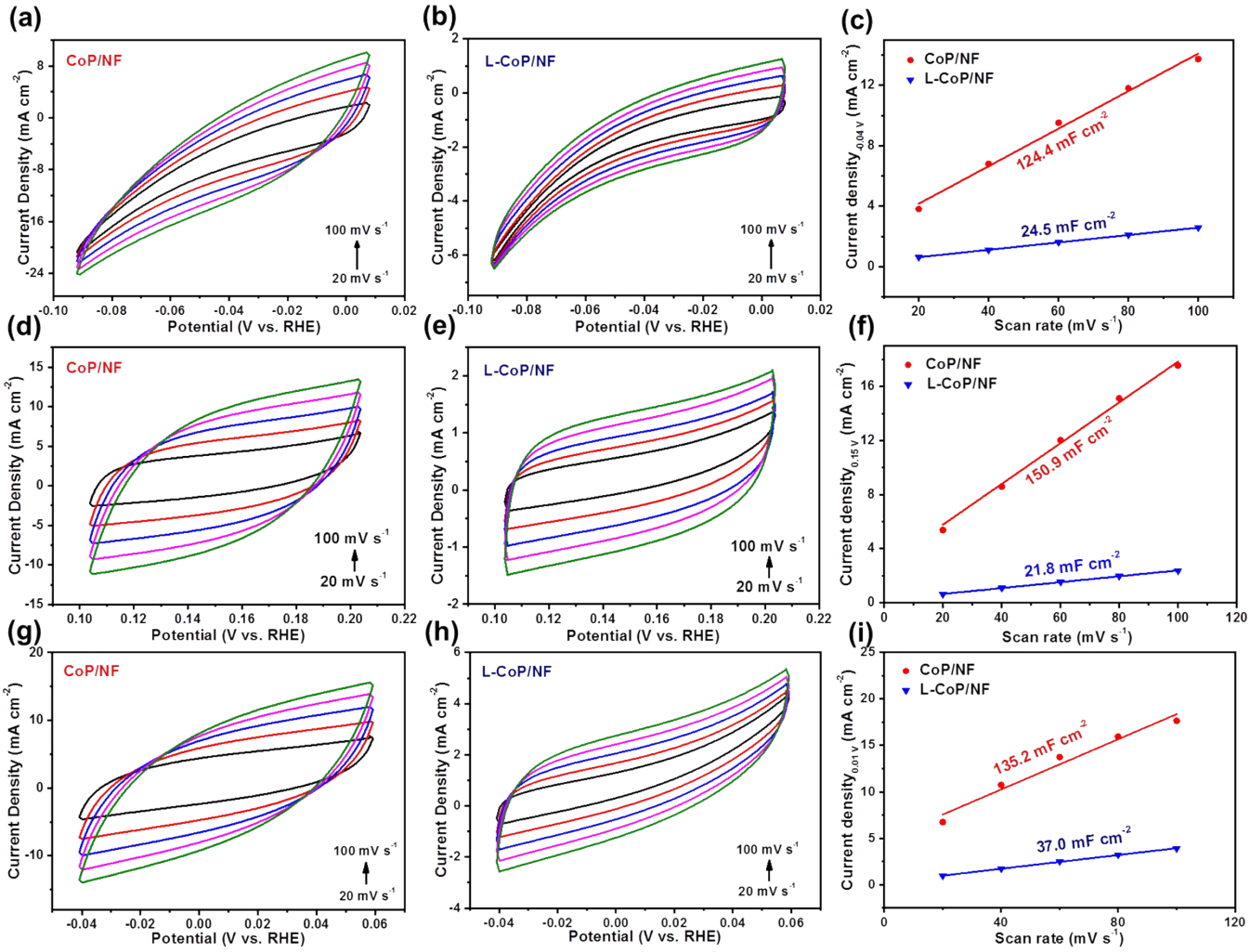

Figure S9. ECSA measurement of CoP/NF and L-CoP/NF catalysts in (a-c) 1 M KOH. (d-f) 1M PBS, (g-i) 0.5 M H_2SO_4. CV curves of (a, d, g) CoP/NF and (b, e, h) L-CoP/NF. (c, f, i) Plots showing the C_{dl} for studied catalysts.

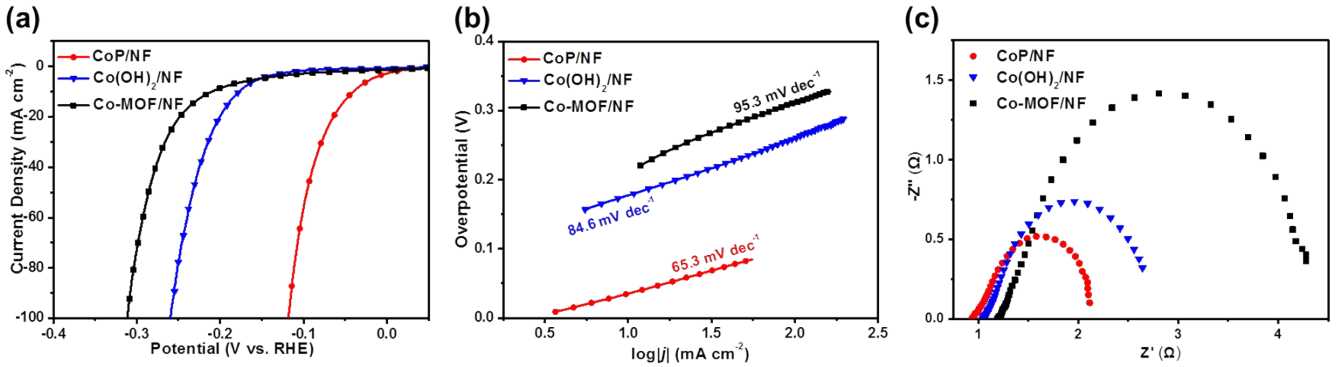

Figure S10. The HER activity of CoP/NF, $Co(OH)_2$/NF and Co-MOF/NF in 1M KOH: (a) LSV curves, (b) Tafel slopes, and (c) Nyquist plots.

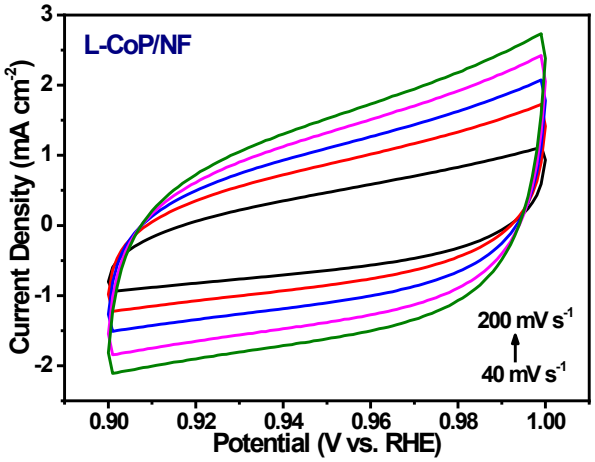

Figure S11. The CV curves at different scan rates of the L-CoP/NF for OER.

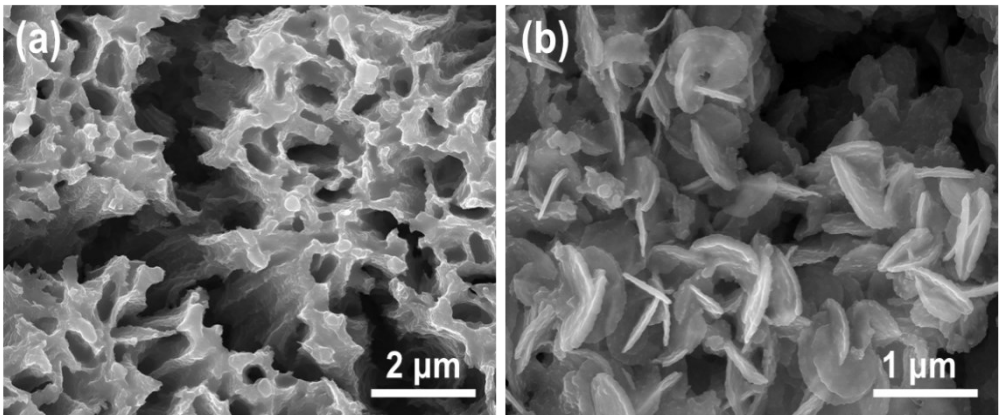

Figure S12. SEM images of cathode material after water electrolysis (Post-HER).

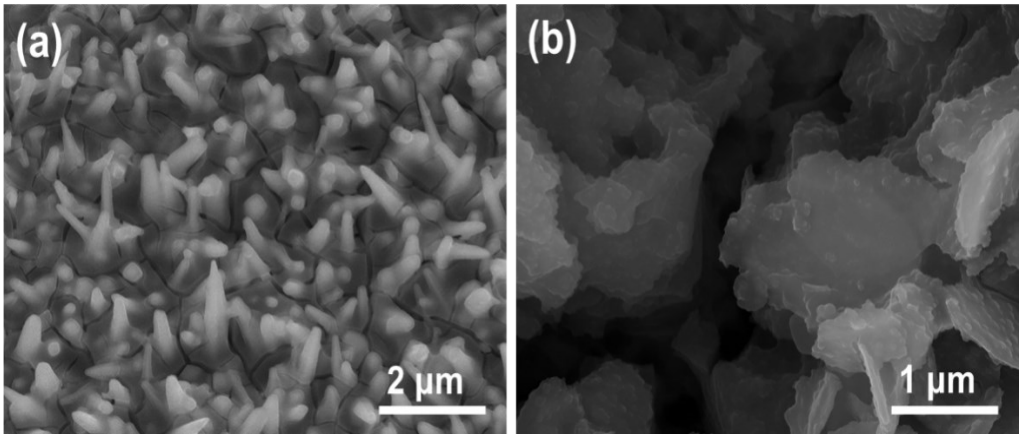

Figure S13. SEM images of anode material after water electrolysis (Post-OER).

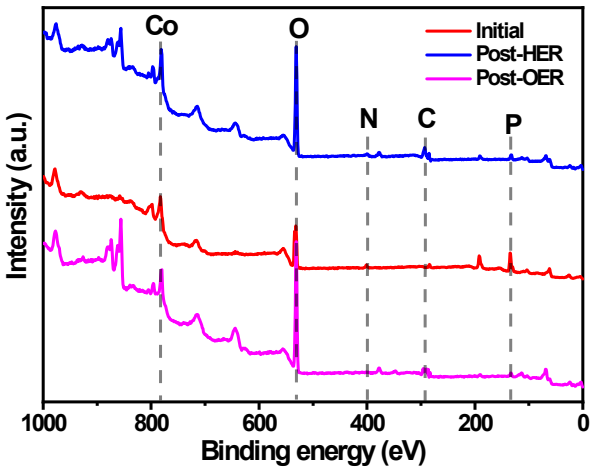

Figure S14. XPS full survey spectra of the CoP/NF after the water electrolysis.

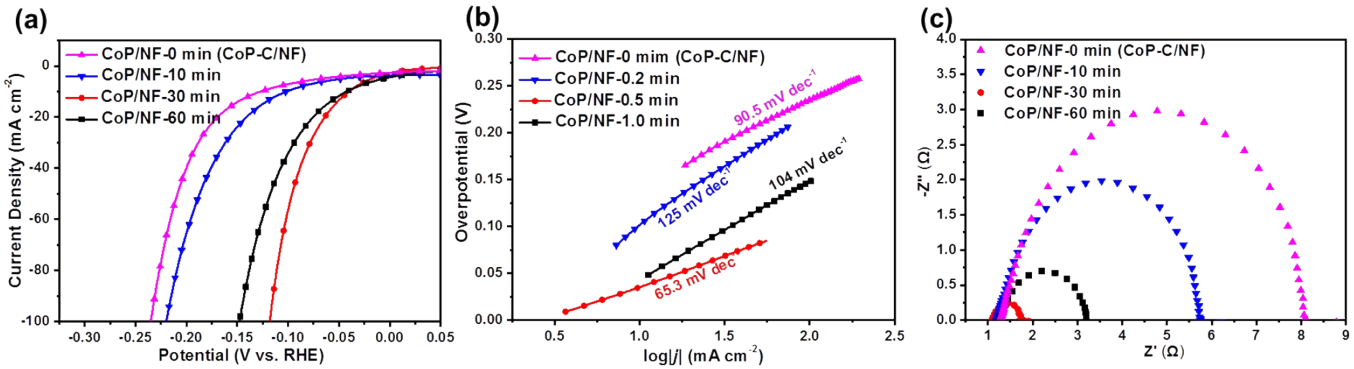

Figure S15. The HER activity of CoP/NF under the different etching time: (a) LSV curves, (b) Tafel slopes and (c) Nyquist plots.

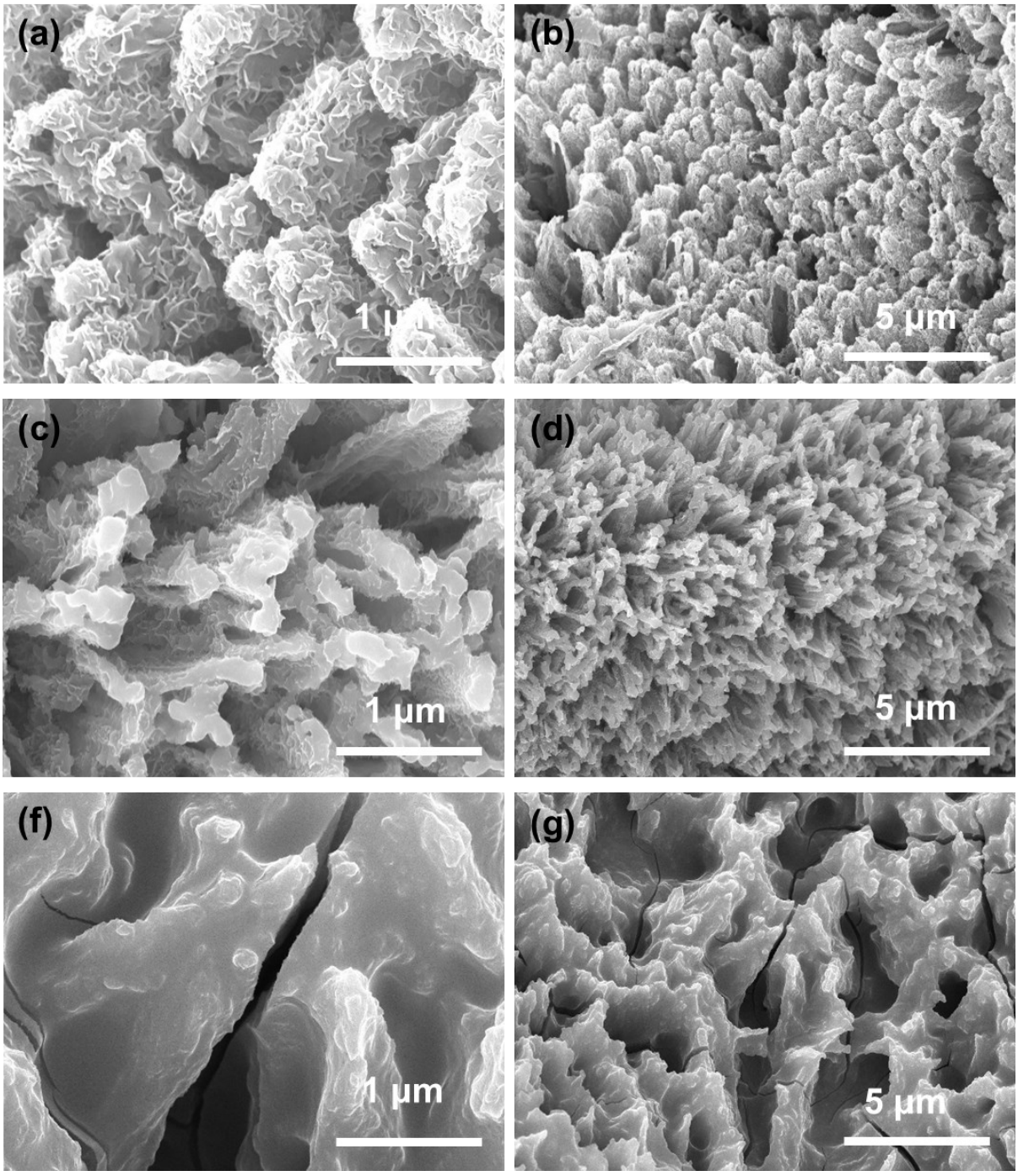

Figure S16. SEM images of CoP/NF under different annealing temperatures: (a, b) 250 °C, (c, d) 300 °C, and (e, f) 350 °C.

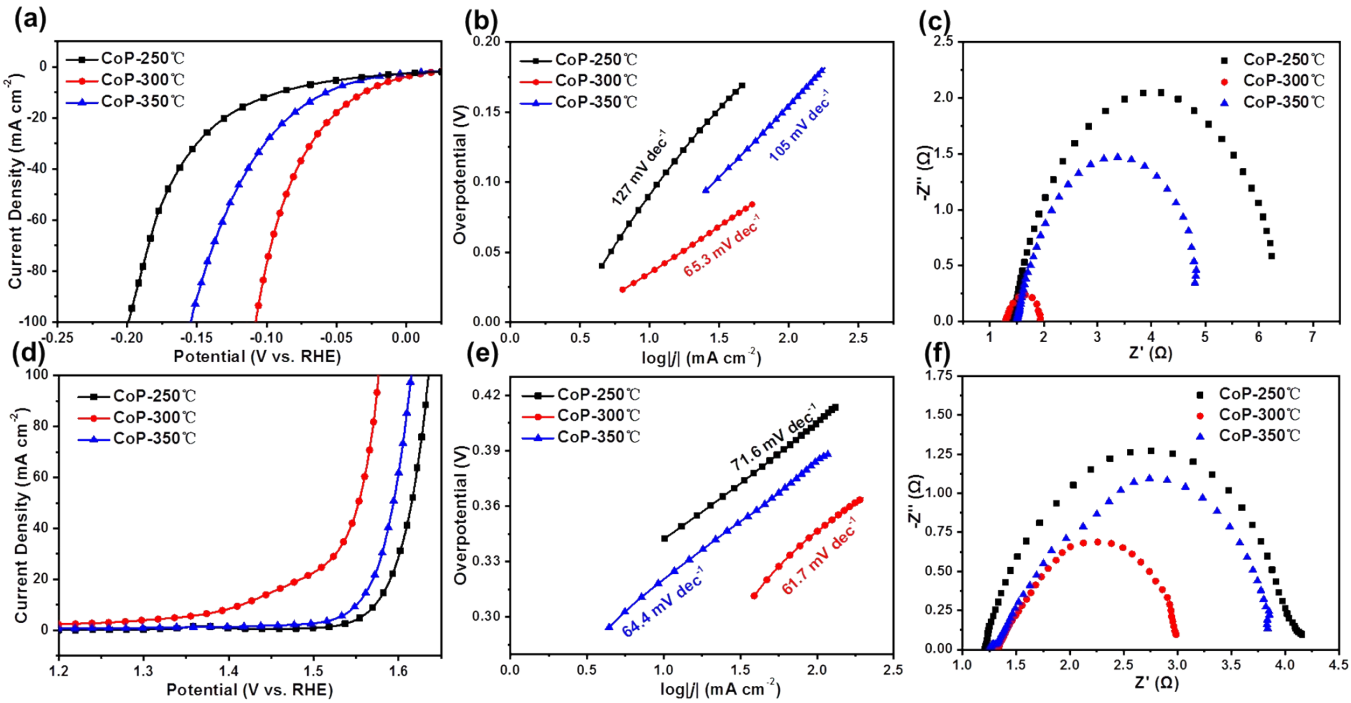

Figure S17. (a, d) LSV curves, (b, e) Tafel slopes and (c, f) Nyquist plots of CoP/NF for HER activity (a-c) and OER activity (d-f) at different annealing temperatures in 1M KOH.

Table S1. Comparison of the HER activity of the CoP/NF with other electrocatalysts previously reported under various pH conditions.

Catalysts	Electrolyte	η_{10}/mV	Tafel slope/mV dec^{-1}	Ref.
CoP/NF	1 M KOH	41.1	65.3	This work
	1 M PBS	55.2	68.7	
	0.5 M H_2SO_4	83.9	55	
CoP/Mo_2C-NC	1 M KOH	67.2	66	1
	1 M PBS	81.8	68	
	0.5 M H_2SO_4	55.7	49	
NFP/C-3	1 M KOH	95	72	2
	1 M PBS	117	70	
	0.5 M H_2SO_4	72	54	
CoP NFs	1 M KOH	136	56.2	3
	1 M PBS	-	-	
	0.5 M H_2SO_4	122	54.8	
CoP/NCNT-CP	1 M KOH	165	96	4
	1 M PBS	305	100	
	0.5 M H_2SO_4	203	56	
NiCo-nitrides/$NiCo_2O_4$/GF	1 M KOH	71	58	5
	1 M KOH	418	78	
	0.5 M H_2SO_4	432	68	
Ni−Co−P−H	1 M KOH	121	65	6
	1 M PBS	157	84	
	0.5 M H_2SO_4	90	68	
CoP NA/CC	1 M KOH	52	58	7
	1 M PBS	145	72	
	0.5 M H_2SO_4	-	-	
MoS_2/EEBP	1 M KOH	237	99	8
	1 M PBS	258	154	
	0.5 M H_2SO_4	126	68	
Mo_2C/N-PC	1 M KOH	100	94.5	9
	1 M PBS	224	140.8	
	0.5 M H_2SO_4	178	72.3	
Co_2Ni_1N	1 M KOH	102.6	60.1	10
	1 M PBS	152.8	90.3	
	0.5 M H_2SO_4	92.0	55.3	
NiCoP/CC	1 M KOH	62	68.2	11
	1 M PBS	-	-	
	0.5 M H_2SO_4	44	38.5	
$CuCo_2$-P	1 M KOH	49.5	58	12
	1 M PBS	62.3	65.6	
	0.5 M H_2SO_4	54.8	42.6	
CoP/Co-MOF	1 M KOH	34	56	13
	1 M PBS	49	63	
	0.5 M H2SO4	27	43	
Ni-Fe-P	1 M KOH	95	72	14
	1 M PBS	117	70	
	0.5 M H_2SO_4	72	54	
Co-Fe-P	1 M KOH	86	66	15
	1 M PBS	138	72	
	0.5 M H_2SO_4	66	138	

Table S2. Comparison of the OER activity of CoP/NF with other electrocatalysts previously reported under

alkaline conditions

Catalysts	Electrolyte	Overpotenial (mV)	Tafel slope/ mV dec^{-1}	Ref.
CoP/NF	1 M KOH	317@50mA cm^{-2}	49	This work
Cu_3NCu_3P/ NPSCNWS@NF	1 M KOH	240@10mA cm^{-2}	53.8	16
NiCoFeP/C	1 M KOH	270@10mA cm^{-2}	65	17
CoP/NCNHP	1 M KOH	310@10mA cm^{-2}	70	18
CoP NA/CC	1 M KOH	300@10mA cm^{-2}	85	7
CoP/rGO-400	1 M KOH	379@20mA cm^{-2}	66	19
Fe-CoP/CoO	1 M KOH	219@10mA cm^{-2}	52	20
Fe_3-NiCoP	1 M KOH	293@50mA cm^{-2}	37.8	21
NiCoP@NC NA/NF	1 M KOH	305@50mA cm^{-2}	70.5	22
NiCoP/CC	1 M KOH	242@10mA cm^{-2}	64.2	11
Co_3O_4/Co-Fe oxide DSNBs	1 M KOH	297@10mA cm^{-2}	61	23
2D Co_3O_4/CBTC	1 M KOH	370@10mA cm^{-2}	50.1	24
Co_4Ni_1P NTS	1 M KOH	245@10mA cm^{-2}	61	25
NiCoP/NC PHCs	1 M KOH	297@10mA cm^{-2}	51	26

Table S3. Comparison of the overall water splitting activity of CoP/NF with other electrocatalysts previously

reported under alkaline conditions

Catalysts	Electrolyte	$\eta_{10,\ overall}$/mV	Ref.
CoP/NF	1 M KOH	1.54	This work
Cu_3NCu_3P/ NPSCNWS@NF	1 M KOH	1.54	16
Co_4Ni_1P NTs	1 M KOH	1.59	25
CoP/NCNHP	1 M KOH	1.64	18
CoP NA/CC	1 M KOH	1.65	7
CoP/rGO-400	1 M KOH	1.7	19
S-CoW@S,N-C	1 M KOH	1.65	27
Fe_3-NiCoP	1 M KOH	1.61	21
CoP NFs	1 M KOH	1.65	3
NiCoP@NC NA/NF	1 M KOH	1.56	22
Co_3O_4/Co-Fe oxide DSNBs	1 M KOH	1.7	23
NiFe-MOF	1 M KOH	1.57	28
AP-$CoFe_2O_4$	1 M KOH	1.63	29
RuNi-NCNFs	1 M KOH	1.56	30
NiFe/$NiCo_2O_4$/NF	1 M KOH	1.67	31
Ni@NC-800	1 M KOH	1.6	32

References:

1 Luo, X.; Zhou, Q.; Du, S.; Li, J.; Zhang, L.; Lin, K.; Li, H.; Chen, B.; Wu, T.; Chen, D.; Chang, M.; Liu, Y., *ACS Appl Mater Interfaces,* 2018, **10**,42335-42347.

2 Lu, X. F.; Yu, L.; Lou, X. W., *Sci. Adv.,* 2019, **5**,eaav6009.

3 Ji, L.; Wang, J.; Teng, X.; Meyer, T. J.; Chen, Z., *ACS Catal.,* 2019, **10**,412-419.

4 Wang, L.; Cao, J.; Cheng, X.; Lei, C.; Dai, Q.; Yang, B.; Li, Z.; Younis, M. A.; Lei, L.; Hou, Y.; Ostrikov, K., *ACS Sustainable Chem. Eng.,* 2019, **7**,10044-10051.

5 Liu, Z.; Tan, H.; Liu, D.; Liu, X.; Xin, J.; Xie, J.; Zhao, M.; Song, L.; Dai, L.; Liu, H., *Adv. Sci.,* 2019, **6**,1801829.

6 Liu, X.; Deng, S.; Xiao, D.; Gong, M.; Liang, J.; Zhao, T.; Shen, T.; Wang, D., *ACS Appl. Mater. Interfaces* 2019, **11**,42233-42242.

7 Liu, T.; Xie, L.; Yang, J.; Kong, R.; Du, G.; Asiri, A. M.; Sun, X.; Chen, L., *ChemElectroChem,* 2017, **4**,1840-1845.

8 Liang, T.; Liu, Y.; Cheng, Y.; Ma, F.; Dai, Z., *ChemCatChem,* 2020, **12**,2840-2848.

9 Han, W.; Chen, L.; Ma, B.; Wang, J.; Song, W.; Fan, X.; Li, Y.; Zhang, F.; Peng, W., *J. Mater. Chem. A,* 2019, **7**,4734-4743.

10 Feng, X.; Wang, H.; Bo, X.; Guo, L., *ACS Appl. Mater. Interfaces,* 2019, **11**,8018-8024.

11 Du, C.; Yang, L.; Yang, F.; Cheng, G.; Luo, W., *ACS Catal.,* 2017, **7**,4131-4137.

12 Cheng, Y.; Pei, Y.; Zhuang, P.; Chu, H.; Cao, Y.; Smith, W.; Dong, P.; Shen, J.; Ye, M.; Ajayan, P. M., *Small,* 2019, **15**,1904681.

13 Liu, T.; Li, P.; Yao, N.; Cheng, G.; Chen, S.; Luo, W.; Yin, Y., *Angew. Chem. Int. Ed.,* 2019, **58**,4679-4684.

14 Ahn, S. H.; Manthiram, A., *J. Mater. Chem. A,* 2017, **5**,2496-2503.

15 Chen, J.; Liu, J.; Xie, J.-Q.; Ye, H.; Fu, X.-Z.; Sun, R.; Wong, C.-P., *Nano Energy,* 2019, **56**,225-233.

16 Wang, Q.; Zhang, Z.; Zhao, X.; Xiao, J.; Manoj, D.; Wei, F.; Xiao, F.; Wang, H.; Wang, S., *ChemElectroChem,* 2020, **7**,289-298.

17 Wei, X.; Zhang, Y.; He, H.; Peng, L.; Xiao, S.; Yao, S.; Xiao, P., *Chem. Commun.,* 2019, **55**,10896-10899.

18 Pan, Y.; Sun, K.; Liu, S.; Cao, X.; Wu, K.; Cheong, W. C.; Chen, Z.; Wang, Y.; Li, Y.; Liu, Y.; Wang, D.; Peng, Q.; Chen, C.; Li, Y., *J. Am. Chem. Soc.,* 2018, **140**,2610-2618.

19 Jiao, L.; Zhou, Y. X.; Jiang, H. L., *Chem. Sci.,* 2016, **7**,1690-1695.

20 Hu, X.; Zhang, S.; Sun, J.; Yu, L.; Qian, X.; Hu, R.; Wang, Y.; Zhao, H.; Zhu, J., *Nano Energy,* 2019, **56**,109-117.

21 Guo, M.; Song, S.; Zhang, S.; Yan, Y.; Zhan, K.; Yang, J.; Zhao, B., *ACS Sustainable Chem. Eng.,* 2020, **8**,7436-7444.

22 Cao, B.; Cheng, Y.; Hu, M.; Jing, P.; Ma, Z.; Liu, B.; Gao, R.; Zhang, J., *Adv. Funct. Mater.,* 2019, **29**,1906316.

23 Wang, X.; Yu, L.; Guan, B. Y.; Song, S.; Lou, X. W. D., *Adv. Mater.,* 2018, **30**,1801211.

24 Zhou, J.; Dou, Y.; Zhou, A.; Shu, L.; Chen, Y.; Li, J.-R., *ACS Energy Lett.,* 2018, **3**,1655-1661.

25 Yan, L.; Cao, L.; Dai, P.; Gu, X.; Liu, D.; Li, L.; Wang, Y.; Zhao, X., *Adv. Funct. Mater.,* 2017, **27**,1703455.

26 Zhang, X.; Huang, L.; Wang, Q.; Dong, S., *J. Mater. Chem. A,* 2017, **5**,18839-18844.

27 Weng, B.; Grice, C. R.; Meng, W.; Guan, L.; Xu, F.; Yu, Y.; Wang, C.; Zhao, D.; Yan, Y., *ACS Energy Lett.,* 2018, **3**,1434-1442.

28 Duan, J.; Chen, S.; Zhao, C., *Nat Commun,* 2017, **8**,15341.

29 Debnath, B.; Parvin, S.; Dixit, H.; Bhattacharyya, S., *ChemSusChem,* 2020, **13**,3875-3886.

30 Li, M.; Wang, H.; Zhu, W.; Li, W.; Wang, C.; Lu, X., *Adv. Sci.,* 2020, **7**,1901833.

31 Xiao, C.; Li, Y.; Lu, X.; Zhao, C., *Adv. Funct. Mater.,* 2016, **26**,3515-3523.

32 Xu, Y.; Tu, W.; Zhang, B.; Yin, S.; Huang, Y.; Kraft, M.; Xu, R., *Adv. Mater.,* 2017, **29**,1605957.